J Stat Phys (2008) 130: 113–128
DOI 10.1007/s10955-007-9446-2

The Percolation Signature of the Spin Glass Transition

J. Machta · C.M. Newman · D.L. Stein

Received: 30 June 2007 / Accepted: 19 September 2007 / Published online: 13 October 2007

Abstract Magnetic ordering at low temperature for Ising ferromagnets manifests itself within the associated Fortuin–Kasteleyn (FK) random cluster representation as the occurrence of a single positive density percolating network. In this paper we investigate the percolation signature for Ising spin glass ordering—both in short-range (EA) and infinite-range (SK) models—within a two-replica FK representation and also within the different Chayes–Machta–Redner two-replica graphical representation. Based on numerical studies of the $\pm J$ EA model in three dimensions and on rigorous results for the SK model, we conclude that the spin glass transition corresponds to the appearance of *two* percolating clusters of *unequal* densities.

Keywords Ising spin glass · Percolation · Graphical representations · Cluster algorithms · Fortuin–Kasteleyn

1 Introduction

Ising type spin glass models, both of the short-range Edward–Anderson (EA) [1] and the infinite-range Sherrington–Kirkpatrick (SK) [2] varieties, have been studied for decades (for some recent reviews, see [3] and [4]). Nevertheless, to a large extent, they remain a mystery—especially the short-range variety, with competing views as to the nature of their

J. Machta (✉)
Physics Department, University of Massachusetts, Amherst, MA 01003, USA
e-mail: machta@physics.umass.edu

C.M. Newman
Courant Institute of Mathematical Sciences, New York University, New York, NY 10012, USA
e-mail: newman@courant.nyu.edu

D.L. Stein
Physics Department and Courant Institute of Mathematical Sciences, New York University, New York, NY 10012, USA
e-mail: daniel.stein@nyu.edu

ordered phases at low temperature T [3–5]. Indeed, from the perspective of rigorous results, it is striking that there is no proof of broken symmetry (e.g., of a nonzero EA order parameter) for any dimension d or temperature T.

Graphical representations such as the Fortuin–Kasteleyn (FK) random cluster model [6, 7] are important tools in the study of spin systems. They relate correlations in spin systems to geometrical properties of associated random graphs. Graphical representations are useful in obtaining rigorous results concerning spin systems (e.g., [8, 9]), they yield geometric insights into the nature of phase transitions and they are the basis for powerful Monte Carlo methods for simulating phase transitions [10–12]. However, graphical representations have, thus far, played a much less important role in the study of spin glasses than they have for ferromagnets.

In this paper, we investigate two different graphical representations—the two-replica graphical representation of Chayes, Machta and Redner (CMR) [13, 14] and a two-replica version of the FK representation (see Sect. 4.1 of [15]). Our purpose is to understand the "percolation signature" of spin glass ordering within these graphical representations. For ferromagnets, ordering corresponds to the occurrence of percolating networks or clusters in the single replica version of the FK representation. As we shall explain, we believe we have elucidated the somewhat more complicated percolation signature for spin glasses.

This should help in understanding better the differences between the nature of the phase transition in ferromagnets and in spin glasses. It is also our hope that for short-range models, this will be a significant step towards developing a rigorous proof for spin glass ordering and eventually lead to a clean analysis of the differences between short- and infinite-range spin glass ordering.

Understanding the percolation signature for spin glasses requires two ingredients beyond what is needed for ferromagnets. The first is the need to consider percolation within a two-replica representation. As mentioned, we consider two different such representations—one is the percolation of a certain class of bonds (these are the "blue bonds" introduced and explained in Sect. 2.2 below) in the CMR two-replica graphical representation and the other is percolation of bonds that are doubly FK occupied—i.e., occupied in *both* replicas—in the two-replica Fortuin–Kasteleyn (TRFK) representation. The two different types of percolation, which we will often refer to simply as CMR and TRFK percolation, give relatively similar (but not identical) results, with the major qualitative distinction occurring within the SK spin glass.

The second ingredient, initially unexpected by us but in retrospect rather natural, is that spin glass ordering corresponds to a more subtle percolation phenomenon than simply the appearance of a percolating cluster—one that involves a pair of percolating clusters. In the case of a ferromagnet, there are general theorems [16] which ensure that when percolation occurs, there is a unique percolating cluster, whether in single or double replica representations. It is also possible (by averaging over disorder realizations) to show (see, e.g., [17] and [15]) that the same conclusions are valid in the single replica FK representation of spin glasses. However for blue bond percolation in the (two-replica) CMR representation of spin glasses, both our numerical evidence for the $d = 3$ EA model and our rigorous results for the SK model (in the CMR representation) show that at temperatures well above the spin glass transition, there already is percolation, but that there are *two* percolating networks which are equal in density (and presumably otherwise macroscopically indistinguishable). The SG transition corresponds to the *breaking of indistiguishability* between the two percolating networks—in particular by having a nonzero difference in densities. The latter feature also occurs for doubly occupied bonds in the TRFK representation of the SK model, except that in that representation there are no percolating networks at all above the transition temperature.

It may be worth noting that a similar breaking of indistinguishability occurs in the homogeneous ferromagnet if one focuses on percolation of *satisfied* bonds (or equivalently, like spins) in a *single* replica. In dimensions three or more at infinite temperature, there are two percolating clusters of equal density (because on those lattices the critical density for independent site percolation is below 1/2). If just below the critical temperature the minority spin percolates within a magnetized phase (and this is rigorously known to occur for sufficiently large d [18]) then there would be two percolating but distinguishable clusters. At the end of Sect. 4, we show some numerical results concerning this phenomenon in the three-dimensional ferromagnet.

From a numerical perspective, spin glasses also pose major challenges. Some of the numerical techniques, e.g., that of Swendsen and Wang (SW) [11] based on graphical representations, such as that of Fortuin and Kasteleyn [6, 7], which have proven so useful for ferromagnets, are in principle applicable to spin glasses. However, they are very inefficient in practice for values of d and T where ordering is believed to occur. The CMR graphical representation is related to a two-replica algorithm originally introduced by Swendsen and Wang [19–21] and developed by these and other authors [22–25]. These authors have shown that algorithms incorporating two-replica cluster moves are somewhat useful in simulating spin glasses. In particular, Jörg [24, 25] has shown that an algorithm based on a two-replica representation performs reasonably efficiently for diluted spin glass models in three dimensions. Two-replica cluster methods have also been successfully applied to Ising systems in a staggered field [14] and to the random field Ising model [26]. The Monte Carlo method that we use takes advantage of the full set of moves allowed by the CMR graphical representation. These moves are a superset of the moves used in [19–21, 23–25].

The paper is organized as follows. In Sect. 2 we introduce the idea of graphical representations, describe the CMR and TRFK two-replica graphical representations and present properties of these representations. In Sect. 3 we analyze both two-replica representations on the complete graph—i.e., for the SK spin glass. In Sect. 4 we present numerical results for the three-dimensional EA model. The paper concludes with a discussion.

2 Graphical Representations for Spin Glasses

2.1 Fortuin–Kasteleyn Graphical Representation

Graphical representations for the Ising model originated with the work of Fortuin and Kasteleyn [6, 7]. They were re-discovered and given a physical interpretation by Coniglio and Klein [27], applied as the basis of a powerful algorithm for simulating the Ising model by Swendsen and Wang [19–21] and then reformulated as a joint spin-bond distribution by Edwards and Sokal [22]. Edwards and Sokal introduced a joint distribution of spin variables $\{\sigma_x\}$ and bond variables $\{\omega_{xy}\}$. Here $\{x\}$ represents the set of sites (vertices) of an arbitrary lattice (graph) and $\{xy\}$ the set of bonds (edges). The Ising spin variables take values ± 1 and the bond variables take values 0 or 1, or "unoccupied" and "occupied", respectively. The statistical weight $\mathcal{W}$ for the Edwards–Sokal distribution is

$$\mathcal{W}(\sigma, \omega; p) = p^{|\omega|}(1-p)^{N_b-|\omega|}\Delta(\sigma, \omega). \tag{1}$$

Here $|\omega| = \sum_{\{xy\}} \omega_{xy}$ is the number of occupied bonds and N_b is the total number of bonds on the lattice. The factor $\Delta(\sigma, \omega)$ is defined by,

$$\Delta(\sigma, \omega) = \begin{cases} 1 & \text{if for every } xy\text{: } \omega_{xy} = 1 \to \sigma_x \sigma_y = 1, \\ 0 & \text{otherwise.} \end{cases} \tag{2}$$

The Δ factor requires that every occupied bond is satisfied. Without the Δ factor we would have independent Bernoulli percolation. Given the choice, $p = \mathcal{P}_{\rm FK}(\beta) = 1 - \exp(-2\beta J)$, it is easy to verify that the spin and bond marginals of the Edwards–Sokal distribution are the ferromagnetic Ising model with coupling strength J and the Fortuin–Kasteleyn random cluster model, respectively.

Bond and spin configurations in the ferromagnet contain essentially the same information. For example, the spin-spin correlation function $\langle \sigma_x \sigma_y \rangle$ is equal to the probability that sites x and y are connected by occupied bonds in the bond representation,

$$\langle \sigma_x \sigma_y \rangle = \text{Prob}\{x \text{ and } y \text{ connected}\}. \tag{3}$$

This relationship implies that the phase transition in the spin system is accompanied by a percolation transition in the bond system.

Given a typical equilibrium bond configuration one can construct a typical equilibrium spin configuration by identifying connected components or clusters and independently populating every spin in each cluster with one randomly chosen spin type. Similarly, given an equilibrium spin configuration, an equilibrium bond configuration can be constructed by occupying satisfied bonds with probability $\mathcal{P}_{\rm FK}(\beta)$. The equivalence between spin and bond configurations is the basis of the Swendsen–Wang algorithm, which proceeds by successively creating spin configurations from bond configurations and then bond configurations from spin configurations. It is easy to verify that this algorithm is ergodic and satisfies detailed balance with respect to the Edwards–Sokal distribution. Power law decay of spin correlations at criticality imply via (3) that the connected components of bond configurations at criticality have a power law distribution of sizes. The efficiency of the Swendsen–Wang algorithm is due to the fact that the spin system is modified on all length scales in a single step.

The FK representation is easily adapted to the $\pm J$ Ising spin glass. (With minor modifications, it can also be adapted to Gaussian and other distributions for the couplings, but we will generally not consider those in this paper.) The corresponding Edwards–Sokal weight is the same as given in (1). The Δ factor must still enforce the rule that all occupied bonds are satisfied,

$$\Delta(\sigma, \omega; J) = \begin{cases} 1 & \text{if for every } xy\text{: } \omega_{xy} = 1 \to J_{xy}\sigma_x\sigma_y = 1, \\ 0 & \text{otherwise.} \end{cases} \tag{4}$$

The spin marginal of the corresponding Edwards–Sokal distribution is the Ising spin glass with couplings $\{J_{xy}\}$. Unfortunately, the relationship between spin-spin correlations and bond connectivity is complicated by the presence of antiferromagnetic bonds. Specifically, one has

$$\begin{aligned} \langle \sigma_x \sigma_y \rangle = {} & \text{Prob}\{x \text{ and } y \text{ connected by even number of antiferromagnetic bonds}\} \\ & - \text{Prob}\{x \text{ and} y \text{ connected by odd number of antiferromagnetic bonds}\}. \end{aligned} \tag{5}$$

It is no longer the case that the percolation of FK bonds implies long range order [28]. Two spins separated by a large distance may usually be connected by occupied bonds but still be uncorrelated because half the time the connection has an even number of antiferromagnetic bonds and half the time an odd number of antiferromagnetic bonds. Indeed, FK bonds percolate at a temperature that is well above the spin glass transition temperature. For the three-dimensional Ising spin glass on the cubic lattice Fortuin–Kasteleyn bonds percolate at $\beta_{{\rm FK},p} \approx 0.26$ [29] while the inverse critical temperature is $\beta_c = 0.89 \pm 0.03$ [30]. Near

the spin glass critical temperature, the giant FK cluster includes most of the sites of the system. For this reason, the Swendsen–Wang algorithm, though valid, is quite inefficient for simulating spin glasses.

2.2 The CMR Two-Replica Graphical Representation

A conceptual difficulty of using the Fortuin–Kasteleyn representation to understand spin glass ordering is that FK clusters identify magnetization correlations but the spin glass order parameter is not the magnetization. Spin glass order is manifest in the Edwards–Anderson order parameter, which can be defined with respect to two independent replicas of the system, each with the same couplings $\{J_{xy}\}$. The spins in the two replicas are $\{\sigma_x\}$ and $\{\tau_x\}$, respectively, each taking values ± 1. The Edwards–Anderson order parameter, q_{EA}, is defined in terms of the overlap,

$$Q = {N_s}^{-1} \sum_{\{x\}} \sigma_x \tau_x, \tag{6}$$

in the limit as the number of sites $N_s \to \infty$. In general, Q is a random variable whose maximum possible value is q_{EA}, but in the case where (in the limit $N_s \to \infty$) $\{\sigma_x\}$ and $\{\tau_x\}$ are drawn from a single pure state, Q takes on only the single value q_{EA}.

The two-replica graphical representation, introduced in [13, 14], explicitly relates spin glass order to geometry. The associated Edwards–Sokal joint distribution has, in addition to the spin variables, $\{\sigma_x\}$ and $\{\tau_x\}$, two types of bond variables ω_{xy} and η_{xy} each taking values in $\{0, 1\}$.

The Edwards–Sokal weight is

$$\mathcal{W}(\sigma, \tau, \omega, \eta; J) = B_{\text{blue}}(\omega) B_{\text{red}}(\eta) \Delta(\sigma, \tau, \omega; J) \Gamma(\sigma, \tau, \eta) \tag{7}$$

where the B's are Bernoulli factors for the two types of bonds,

$$B_{\text{blue}}(\omega) = \mathcal{P}_{\text{blue}}^{|\omega|} (1 - \mathcal{P}_{\text{blue}})^{N_b - |\omega|}, \tag{8}$$

$$B_{\text{red}}(\eta) = \mathcal{P}_{\text{red}}^{|\eta|} (1 - \mathcal{P}_{\text{red}})^{N_b - |\eta|} \tag{9}$$

and the bond occupation probabilities are

$$\mathcal{P}_{\text{blue}} = 1 - \exp(-4\beta |J|), \tag{10}$$

$$\mathcal{P}_{\text{red}} = 1 - \exp(-2\beta |J|). \tag{11}$$

The Δ and Γ factors constrain where the two types of occupied bonds are allowed,

$$\Delta(\sigma, \tau, \omega; J) = \begin{cases} 1 & \text{if for every } xy\text{: } \omega_{xy} = 1 \to J_{xy} \sigma_x \sigma_y > 0 \text{ and } J_{xy} \tau_x \tau_y > 0, \\ 0 & \text{otherwise,} \end{cases} \tag{12}$$

$$\Gamma(\sigma, \tau, \eta) = \begin{cases} 1 & \text{if for every } xy\text{: } \eta_{xy} = 1 \to \sigma_x \sigma_y \tau_x \tau_y < 0, \\ 0 & \text{otherwise.} \end{cases} \tag{13}$$

We refer to the ω occupied bonds as "blue" and the η occupied bonds as "red". The Δ constraint says that blue bonds are allowed only if the bond is satisfied in both replicas. The Γ constraint says that red bonds are allowed only if the bond is satisfied in exactly one replica.

It is straightforward to verify that the spin marginal of the CMR Edwards–Sokal weight is the weight for two independent Ising spin glasses with the same couplings,

$$\sum_{\{\omega\}\{\eta\}} \mathcal{W}(\sigma, \tau, \omega, \eta; J) = \text{const} \times \exp\left[\beta \sum_{\{xy\}} J_{xy}(\sigma_x \sigma_y + \tau_x \tau_y)\right]. \tag{14}$$

2.3 Properties of Graphical Representations for Spin Glasses

Connectivity by occupied bonds in the CMR representation is related to correlations of the local spin glass order parameter,

$$Q_x = \sigma_x \tau_x. \tag{15}$$

It is straightforward to verify that

$$\begin{aligned}\langle Q_x Q_y \rangle = &\text{Prob}\{x \text{ and } y \text{ connected by even number of red bonds}\} \\ &- \text{Prob}\{x \text{ and } y \text{ connected by odd number of red bonds}\}.\end{aligned} \tag{16}$$

As in the case of the FK representation, a minus sign complicates the relationship between correlations and connectivity but in a conceptually different way. The second term in (16) is independent of the underlying coupling in the model and is present for both spin glasses and ferromagnetic models.

In the case of a ferromagnet, having a percolating cluster (or clusters) in the (single replica) FK representation easily shows that there is broken symmetry with respect to global spin flips. For example, one can impose plus or minus boundary conditions on those boundary spins belonging to FK percolating networks in the Edwards–Sokal joint spin-bond representation and these two choices of boundary conditions give two different Gibbs states for the spin system in the infinite volume limit. More simply, in the ferromagnetic case, the magnetization order parameter equals the total density of the percolating network(s), since finite FK clusters do not contribute.

We remark, as noted in Sect. 1, that for ferromagnets (in the absence of boundary conditions that force interfaces), the signature of ordering is a *single* percolating cluster. For spin glasses, the situation is analogous, but more complicated. If there is in the CMR graphical representation a percolating blue cluster of strictly larger density than any other blue clusters, one can similarly show broken symmetry. Here one can impose "agree" or "disagree" boundary conditions between those σ_x and τ_x boundary spins belonging to the maximum density blue network.[1] In the infinite volume limit, these two boundary conditions give different Gibbs states for the σ-spin system (for fixed τ) related to each other by a global spin flip (of σ). However, in this case, it is not so easy to rigorously relate (in general) the overlap Q to the densities of percolating blue networks, even if one assumes that there are exactly two such networks with densities D_1 and D_2. This is because in a two-replica situation, it is not immediate that there is no contribution from finite (non-percolating) clusters, which would be enough to imply that $Q = D_1 - D_2$. Nevertheless, this identity seems likely to be the case, and indeed is valid for the SK model, as we discuss in the next section of the paper.

For the TRFK representation, similar reasoning shows that the occurrence of exactly two doubly-occupied percolating FK clusters with different densities implies broken symmetry

[1] We remark that this is indeed a *boundary* condition because, in the infinite volume limit, determining which boundary spins belong to the maximum density network does not use information from any fixed, arbitrarily large, finite region.

for the spin system [15] and that Q should equal (and does equal in the SK model) the density difference. In Sect. 4.3 we will present preliminary numerical evidence that there is such a nonzero density difference below the spin glass transition temperature for the $d = 3$ EA $\pm J$ spin glass (for both the TRFK and CMR representations).

3 The Spin Glass on the Complete Graph

The spin glass on the complete graph was introduced by Sherrington and Kirkpatrick (SK) [2]. The $\pm J$ version of the model has couplings given by $\pm N^{-1/2}$ where N is the number of vertices on the graph. This scaling for the coupling strength insures that the free energy is extensive. In this section, we study the percolation properties of both the Fortuin–Kasteleyn and CMR representations for the SK model. In the high temperature phase, $\beta < \beta_c = 1$, both the magnetization and the EA order parameter, q_{EA}, vanish. The SK solution, valid for the high temperature phase, yields the energy per spin, $u = -\beta/2$. The number of unsatisfied edges minus the number of satisfied edges is equal to $uN^{3/2}$. Thus, letting f_s be the fraction of satisfied edges, we have that

$$f_s \sim \frac{1}{2} - uN^{-1/2}. \tag{17}$$

In the FK representation a fraction $\mathcal{P}_{\mathrm{FK}} = 1 - \exp(-2\beta N^{-1/2}) \approx 2\beta N^{-1/2}$ of satisfied edges are occupied. When will the occupied edges first form a giant cluster and how many giant clusters will coexist? The theory of random graphs (see [31]) can be used to answer these questions. It is known [32] that a giant cluster forms in a random graph of N vertices when a fraction x/N of edges is occupied with $x > 1$, and that there is then a single giant cluster. This suggests that (single replica) FK giant clusters should form with $\beta = xN^{-1/2}$ when $x > 1$, i.e., that the single replica FK percolation threshold is at

$$\beta_{\mathrm{FK},p} = N^{-1/2}. \tag{18}$$

It also suggests that above this threshold, there should be a single giant FK cluster.

Although the arguments just given are incomplete in that the satisfied edges were treated (without justification) as though they were chosen independently of each other, nevertheless the conclusions can be proved rigorously as we now explain. Indeed, our rigorous analysis of the much more interesting cases with two replicas will use very similar arguments. The idea is to obtain upper and lower bounds for the conditional probability that an edge $\{x_0 y_0\}$ is satisfied, given the satisfaction status of all the other edges. If these bounds are close to each other (for large N) then treating the satisfied edges as though chosen independently can be justified.

A key point is that because of frustration, such approximate independence is impossible if one knows too much about the signs of the couplings. Thus, we will *not* condition on the sign of the single coupling $J_{x_0 y_0}$—in fact we will consider precisely the conditional probability of that sign given the configuration of all other couplings J_{xy} and all spins σ_x. For the $\pm J$ model that we are considering, it is quite elementary to see first that the ratio Z_+/Z_- for the partition functions with $J_{x_0 y_0} = +N^{-1/2}$ and $J_{x_0 y_0} = -N^{-1/2}$ satisfies

$$\exp(-2\beta N^{-1/2}) \le |Z_+/Z_-| \le \exp(2\beta N^{-1/2}), \tag{19}$$

and then that the conditional probabilities $P_\pm$ that $J_{x_0y_0} = \pm N^{-1/2}$ given any configuration of the other J_{xy}'s and all σ_x's satisfy

$$e^{-4\beta/\sqrt{N}} \le e^{-2\beta/\sqrt{N}}|Z_-/Z_+| \le P_+/P_- \le e^{2\beta/\sqrt{N}}|Z_-/Z_+| \le e^{4\beta/\sqrt{N}}. \tag{20}$$

It then follows that the conditional probabilities P_s or P_u for any edge $\{x_0y_0\}$ to be satisfied or unsatisfied given the satisfaction status of all other edges satisfy

$$e^{-4\beta/\sqrt{N}} \le P_s/P_u \le e^{4\beta/\sqrt{N}}, \tag{21}$$

so that

$$\frac{1}{2} - \mathrm{O}(\beta/\sqrt{N}) = (e^{4\beta/\sqrt{N}} + 1)^{-1} \le P_s \le (e^{-4\beta/\sqrt{N}} + 1)^{-1} = \frac{1}{2} + \mathrm{O}(\beta/\sqrt{N}). \tag{22}$$

One now obtains rigorously the same conclusions as before—i.e., (18) is valid with a single giant FK cluster for $\beta = \beta_N \ge xN^{-1/2}$ with any $x > 1$. Before proceeding to our detailed analysis of the situation with two replicas, we state our main conclusions.

The threshold for TRFK percolation is

$$\beta_{\mathrm{TRFK},p} = 1. \tag{23}$$

For $\beta \le 1$, there is no giant cluster (containing a strictly positive density, i.e., fraction of sites). For $\beta > 1$ there are exactly two giant clusters with unequal densities. (Strictly speaking, we do not rigorously rule out the possibility that for some choices of $\beta > 1$, there might be only a single giant cluster, but we explain why that should not be so and also prove that a nonzero spin-spin overlap rules out the possibility of two clusters of exactly equal density.)

The threshold for percolation of blue bonds in the CMR two-replica graphical representation is

$$\beta_{\mathrm{CMR},p} = N^{-1/2}. \tag{24}$$

Only above that threshold are there one or more giant clusters. The number and density of the giant clusters is determined by a second threshold which is exactly the SK spin glass critical value $\beta_c = 1$. For $xN^{-1/2} \le \beta_N \le 1$ with $x > 1$, there are exactly two giant clusters, which have equal densities; if $N^{1/2}\beta_N \to \infty$, then the two densities are both exactly $1/2$. For $\beta_N \ge x$ with any $x > 1$, there are two giant clusters of unequal densities, whose sum is one. (Strictly speaking, as in the case of TRFK percolation, we do not rigorously rule out the possibility that for some $\beta > 1$, there might be a single blue giant cluster, which would necessarily have density one.)

Now we explain our analysis when there are two spin replicas σ and τ. For both TRFK percolation and for blue percolation in the CMR graphical representation, we focus on *doubly satisfied* edges. For the Fortuin–Kasteleyn representation, doubly satisfied edges are occupied with probability $\mathcal{P}_{\mathrm{TRFK}} = [1 - \exp(-2\beta N^{-1/2})]^2 \sim 4\beta^2/N$. For the CMR representation, doubly satisfied edges are occupied with probability $\mathcal{P}_{\mathrm{CMR}} = 1 - \exp(-4\beta N^{-1/2}) \sim 4\beta N^{-1/2}$. The crucial new ingredient in two-replica situations is that an edge $\{xy\}$ can be doubly satisfied only if $\sigma_x\sigma_y\tau_x\tau_y = +1$ or equivalently if $\sigma_x\tau_x = \sigma_y\tau_y$ (and then will be satisfied for exactly one of the two signs of J_{xy}). Thus, before proceeding as in the single replica situation, we first divide all (σ, τ) configurations into two groups or sectors—the *agree* (where $\sigma_x = \tau_x$) and the *disagree* sectors (where $\sigma_x = -\tau_x$). We also denote by N_a

and N_d the numbers of sites in the sectors and denote by $D_a = N_a/N$ and $D_d = N_d/N$ the sector densities (so that $D_a + D_d = 1$). We note that the spin overlap Q is just

$$Q = \frac{1}{N}\sum_x \sigma_x \tau_x = \frac{N_a - N_d}{N} = D_a - D_d \tag{25}$$

and that for $\beta \le \beta_c = 1$, $Q \to 0$ as $N \to \infty$ while for $\beta > \beta_c = 1$, Q is nonzero, e.g., in the sense that $Av(\langle Q^2\rangle) > 0$ as $N \to \infty$, where Av denotes the average over couplings.

We now proceed similarly to the single replica case, but separately within the agree and disagree sectors. Letting $\bar{P}_\pm$ denote the conditional probabilities that $J_{x_0y_0} = \pm N^{-1/2}$ given the other J_{xy}'s and all σ_x's and τ_x's, we have within either of the two sectors that

$$e^{-8\beta/\sqrt{N}} \le e^{-4\beta/\sqrt{N}}|Z_-/Z_+|^2 \le \bar{P}_+/\bar{P}_- \le e^{4\beta/\sqrt{N}}|Z_-/Z_+|^2 \le e^{8\beta/\sqrt{N}} \tag{26}$$

so that the conditional probability *within a single sector* P_{ds} for x_0y_0 to be doubly satisfied is $(1/2) + \mathrm{O}(\beta N^{-1/2})$. For $\beta \le \beta_c$, we have $D_a = 1/2$, $D_d = 1/2$ (in the limit $N \to \infty$) and so in either sector, double FK percolation is approximately a random graph model with $N/2$ sites and bond occupation probability $(1/2)4\beta^2 N^{-1} = \beta^2(N/2)^{-1}$; thus double FK giant clusters do not occur for $\beta^2 \le 1$.

Blue percolation corresponds to bond occupation probability $(1/2)4\beta N^{-1/2} = \beta N^{1/2} \times (N/2)^{-1}$ and so the threshold for blue percolation is given by (24). But now there are *two* giant clusters, one in each of the two sectors, and they are of equal density for $\beta \le \beta_c = 1$ since $D_a = D_d$. On the other hand, for $\beta > \beta_c$, $D_a \ne D_d$ and the two giant clusters will be of unequal density. In fact, since $\beta N^{1/2} \to \infty$ for $\beta > \beta_c$ (indeed for any fixed $\beta > 0$), it follows from random graph theory that each giant cluster occupies the entire sector so that D_a and D_d are also the cluster percolation densities of the two giant clusters.

In the case of two-replica FK percolation for $\beta > \beta_c$, let us denote by $D_{\max}$ and $D_{\min}$ the larger and smaller of D_a and D_d, so that $D_{\max} + D_{\min} = 1$ and $D_{\max} - D_{\min} = Q$. Then for $\beta > \beta_c$, the bond occupation probability in the larger sector is $\beta^2(N/2)^{-1} = 2\beta^2 D_{\max}(D_{\max}N)^{-1}$ with $2\beta^2 D_{\max} > 1$ and there is a (single) giant cluster in that larger sector. There will be another giant cluster (of lower density) in the smaller sector providing $2\beta^2 D_{\min}$ $(= \beta^2(1 - Q)) > 1$. Since $Q \le q_{EA}$, for this to be the case it suffices if for $\beta > \beta_c$,

$$q_{EA} < 1 - \frac{1}{\beta^2}. \tag{27}$$

The estimated behavior of q_{EA} both as $\beta \to 1+$ and as $\beta \to \infty$ [5] suggests that this is always valid. In any case, we have proved that there is a unique maximal density double FK cluster for $\beta > \beta_c$.

4 Numerical Simulations

In this section we describe numerical simulations of the Edwards–Anderson spin glass in three dimensions to test ideas about the percolation signature for spin glass ordering. For comparison, we also describe simulations of spin clusters for the $3D$ ferromagnetic Ising model.

4.1 Methods

We carried out simulations of the $\pm J$ Ising spin glass using a Monte Carlo method that combines CMR cluster moves, Metropolis sweeps and parallel tempering (replica exchange). A similar scheme was used in a study of the random field Ising model [26]. The cluster moves are closely related to the replica Monte Carlo algorithm introduced by Swendsen and Wang [19–21] and developed in [23–25]. The combination of two-replica cluster moves and parallel tempering was first introduced by Houdayer [23]. The new ingredient in the present algorithm is that all of the degrees of freedom available in the CMR representation are used. The additional degree of freedom is incorporated in "grey" moves, described below.

The parallel tempering component of the algorithm works with R pairs of replicas at equally spaced inverse temperatures. Standard temperature exchange moves are carried out between one of the two replicas at one temperature and at one of the neighboring temperatures. The CMR cluster moves begin by identifying all singly and doubly satisfied bonds and occupying them with probabilities, $\mathcal{P}_{\text{blue}} = 1 - \exp(-4\beta)$ and $\mathcal{P}_{\text{red}} = 1 - \exp(-2\beta)$, respectively. Bonds that are not satisfied in either replica cannot be occupied. The occupied bonds determine blue and grey clusters. Sets of sites connected by blue bonds and singletons are considered to be blue clusters. Sets of sites connected by blue or red bonds are considered to be grey clusters. The cluster moves proceed as follows. For each grey cluster a random bit determines whether to perform a grey move or not. If a grey move is chosen, the sign of Q in each blue cluster in the grey cluster is reversed. Next, a random bit determines which of the two spin states to put each blue cluster in given its Q state. For example, if $Q = 1$ in a given blue cluster then, with equal probability, the spin state of a given site in the cluster is either $(++)$ or $(--)$.

The two-replica cluster component of the algorithm satisfies detailed balance with respect to the Edwards–Sokal weight for the CMR graphical representation. In addition, the two-replica cluster component of the algorithm is, by itself, ergodic. There is a non-vanishing probability that any given site is a singleton cluster and is flipped to any of the four spin states. Thus, there is a non-vanishing probability of a transition from any spin configuration for the pair of replicas to any other spin configuration in a finite number of steps. A single pair of replicas will eventually approach equilibrium under two-replica cluster moves. However, for reasons that will become clear in Sect. 4.3, the equilibration by two-replica cluster moves alone is very slow in three dimensions. Thus we supplement these moves with both temperature exchange moves and Metropolis sweeps.

The presence of very long-lived metastable states makes it difficult to gauge whether a spin glass simulation has reached equilibrium. Here we measure the time it takes for a spin configuration, originally at the highest simulated temperature, to diffuse by replica exchange moves, to the lowest temperature. If the entire set of replicas is in equilibrium and if the replica pair at the highest temperature is rapidly equilibrated, then this first passage time estimates the time it takes to obtain an independent sample at the lowest temperature. We assume that the mean first passage time is comparable to the equilibration time for the full set of replicas though it is conceivable that equilibration time is much longer than the mean first passage time. For the 12^3 system, the largest system studied here, the mean first passage time is of the order of one hundred MC sweeps and does not vary greatly from one realization to another so we believe that the system is well equilibrated.

The two-replica cluster moves complicate the ability to keep track of a single spin configuration as it diffuses in temperature space. If there are two giant clusters and, in one of the replicas, both or neither of the giant clusters are flipped then the identity of the spin configuration is unaffected (though it may have suffered an overall spin flip). On the other hand, if

one giant cluster is flipped and the other not then the spin configurations of the replicas are swapped. Below the CMR percolation transition, this same rule is applied to the two largest clusters but the identity of the spin configuration is effectively lost in one two-replica move.

4.2 Improved Estimators

One advantage of cluster algorithms in data collection is the existence of improved estimators [12] in the graphical representation. For example, in the Swendsen–Wang algorithm, one can obtain the magnetization and magnetic susceptibility from the cluster configurations. The magnetization is the average size of the largest cluster and the susceptibility is proportional to the sum of the squares of the cluster sizes. Since each occupied bond configuration corresponds to many spin configurations, the variance of observables measured from the bond configurations is less than for the same observables measured in the spin configuration leading to smaller error bars for the same amount of computational work. Improved estimators exist within the CMR representation for the spin glass order parameter and susceptibility. For example, the order parameter Q can be obtained from the percolating grey cluster if it exists and is unique. In particular, the local order parameter Q_x summed over the sites of the percolating grey cluster should equal the Q of the whole system since the contributions of small grey clusters vanishes after averaging over the possible spin states of these clusters.

4.3 Simulation results

We simulated the three-dimensional $\pm J$ Edwards–Anderson model on skew periodic cubic lattices for system sizes 6^3, 8^3, 10^3 and 12^3. For each size we simulated 20 inverse temperatures equally spaced in the range $\beta = 0.16$ to $\beta = 0.92$. Since there are two replicas for each temperature, the total number of replicas simulated was 40. A recent estimate of the phase transition temperature of the system is $\beta_c = 0.89 \pm 0.03$ [30]. For each size we simulated 100 realizations of disorder for 50,000 Monte Carlo sweeps of which the first $1/4$ of the sweeps were for equilibration and the remaining $3/4$ for data collection. One Monte Carlo sweep consists of a cluster move for the pair of replicas at every temperature, a Metropolis sweep for each replica and a temperature exchange attempt for each temperature. The quantities that we measure are the fraction of sites in the largest blue cluster, $\mathcal{C}_1$ and second largest blue cluster, $\mathcal{C}_2$ and the number of blue CMR wrapping cluster, w_{CMR}, and the number of TRFK "wrapping" clusters, w_{TRFK}. A cluster is said to wrap if it is connected around the system in any of the three directions.

Figure 1 shows the average number $\overline{w_{\mathrm{CMR}}}$ of CMR blue wrapping clusters as a function of inverse temperature β. The curves are ordered by system size with largest size on the bottom

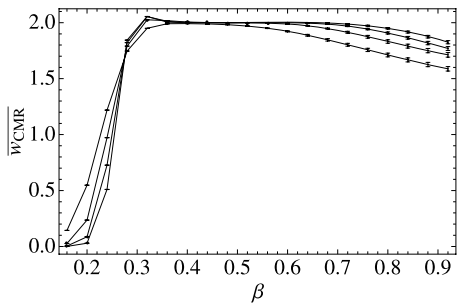

Fig. 1 Average number of wrapping CMR clusters, $\overline{w_{\mathrm{CMR}}}$ vs. β for the 3D EA model

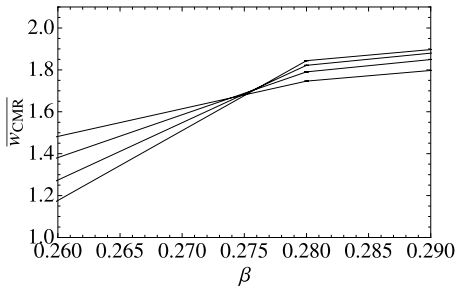

Fig. 2 Same as Fig. 1, magnified near the CMR percolation transition

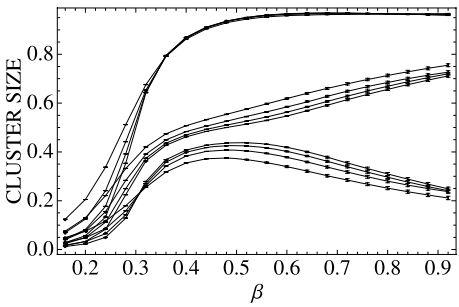

Fig. 3 $\mathcal{C}_1$ (*middle set*), $\mathcal{C}_2$ (*bottom set*) and $\mathcal{C}_1 + \mathcal{C}_2$ (*top set*) vs. β for the CMR graphical representation for the 3D EA model

for the small β and on top for the large β. The data suggests that there is a percolation transition at some $\beta_{\mathrm{CMR},p}$. For $\beta > \beta_{\mathrm{CMR},p}$ there are *two* wrapping clusters while for $\beta < \beta_{\mathrm{CMR},p}$ there are none. Near and above the spin glass transition at $\beta_c \approx 0.89$ the expected number of wrapping clusters falls off but the fall-off diminishes as system size increases. This figure suggests that in the large size limit there are exactly two spanning clusters near the spin glass transition both above and below the transition temperature. Figure 2 is a magnification of Fig. 1 near the CMR percolation transition. The crossing points identify the percolation transition as $\beta_{\mathrm{CMR},p} \approx 0.275$. This value is close to the FK percolation transition for the $\pm J$ EA model $\beta_{\mathrm{FK},p} \approx 0.26$ reported in [29]. A more careful study would be needed to test the hypothesis that $\beta_{\mathrm{CMR},p} > \beta_{\mathrm{FK},p}$.

Figure 3 shows the fraction of sites in the largest CMR blue cluster, $\mathcal{C}_1$, second largest CMR blue cluster, $\mathcal{C}_2$ and the sum of the two, $\mathcal{C}_1 + \mathcal{C}_2$. The middle set of four curves is $\mathcal{C}_1$ for sizes 6^3, 8^3, 10^3 and 12^3, ordered from top to the bottom at $\beta = 0.5$. The bottom set of curves is $\mathcal{C}_2$ with system sizes ordered from smallest on bottom to largest on top at $\beta = 0.5$. The difference between the fraction of sites in the two largest clusters, $\mathcal{C}_1 - \mathcal{C}_2$ is approximately the spin glass order parameter. As the system size increases, this difference decreases below the transition suggesting that $\mathcal{C}_1 = \mathcal{C}_2$ for $\beta < \beta_c$ in the thermodynamic limit. On the other hand, the sum of the two largest clusters is quite constant independent of system size. Near the transition, approximately 96% of the sites are in the two largest clusters.

The large fraction of sites in the two largest clusters makes the CMR cluster moves inefficient. If all sites were in the two largest clusters then the cluster moves would serve only to flip all spins in one or both clusters or exchange the identity of the two replicas. Equilibration depends on the small fraction of spins that are not part of the two largest clusters. One of the reasons that bond diluted spin glasses are more efficiently simulated using two-replica cluster algorithms is the smaller fraction of sites in the two largest clusters. We have carried out simulations on the same bond diluted Ising spin glass studied by Jörg [24, 25]. This model has 55% of the couplings set to zero and 45% set to ± 1. Near the phase transition,

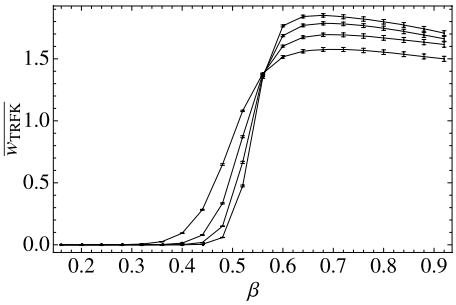

Fig. 4 Average number of doubly occupied wrapping Fortuin–Kasteleyn clusters, $\overline{w_{\mathrm{TRFK}}}$ vs. β for the 3D EA model

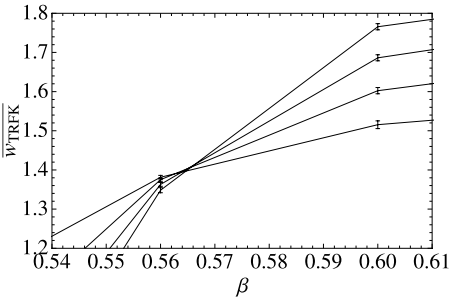

Fig. 5 Same as Fig. 4, magnified near the TRFK percolation transition

we find that only 87% of the sites are contained in the two largest clusters instead of the 96% found in the undiluted spin glass.

Figure 4 show the average number of wrapping TRFK clusters $\overline{w_{\mathrm{TRFK}}}$ as a function of inverse temperature. The largest system size is on the bottom for the small β and on top for the large β. As for the case of CMR clusters, the data suggests a transition at some $\beta_{\mathrm{TRFK},p}$ from zero to two wrapping TRFK clusters. Although the number of TRFK wrapping clusters is significantly less than two for all β and all system sizes, the trend in system size suggests that it might approach two for large systems and $\beta > \beta_{\mathrm{TRFK},p}$. Figure 5 shows a close up of the transition region and the crossing points give the inverse percolation temperature as $\beta_{\mathrm{TRFK},p} \approx 0.565$.

The percolation signature for both CMR and TRFK clusters is qualitatively similar in three dimensions. In both cases two giant clusters with opposite values of the local order parameter appear at a temperature substantially above the phase transition temperature. In the high temperature phase, the two giant clusters have the same density and the phase transition is marked by the onset of different densities of the two clusters. This scenario is not unlike what is expected in the ferromagnetic Ising model for the graph defined by satisfied bonds. On the cubic lattice in the high temperature phase we expect two giant clusters of up and down spins of equal density. The ferromagnetic Ising phase transition is marked by the onset of different densities of the two clusters. Figure 6 shows the largest and second largest cluster of satisfied bonds and the sum of the two for the ferromagnetic Ising model. The system sizes are the same as for the spin glass simulations: 6^3, 8^3, 10^3 and 12^3. The vertical axis is located at the critical temperature. This figure is qualitatively similar to the results for the two largest clusters in the CMR representations. In both cases, for these system sizes, the phase transition is quite rounded in the sense that a difference in density develops well before the transition and the transition itself cannot be identified by looking at the size of the clusters. The difference in the density of the two clusters is thus not a sharp indicator of the phase transition for small system sizes.

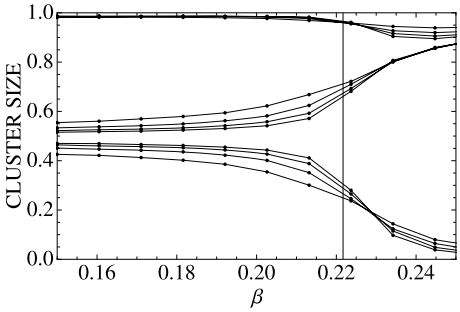

Fig. 6 The size of the largest cluster of satisfied bonds (*middle set*), the second largest cluster (*bottom set*) and the sum of the two largest clusters (*top set*) vs. β for the three-dimensional ferromagnetic Ising model

5 Discussion

In this paper we have proposed a new percolation-theoretic approach towards understanding the nature of the spin glass phase transition. It is based on the Fortuin–Kasteleyn [6, 7] random cluster method (and some variants), which has been enormously useful in analyzing phase transitions in ferromagnets, but had much less impact on systems such as spin glasses until now (see, however, [20, 24, 25]).

There are a number of advantages to our approach. First, and most obviously, it sheds new light on the nature of the spin glass phase transition, particularly its geometric aspects. For example, it provides at least a qualitative explanation of why the EA spin glass on a simple planar lattice doesn't have broken spin flip symmetry at positive temperature (see below). Second, it indicates a possible new framework towards an eventual rigorous proof of an EA spin glass phase transition (at least in sufficiently high dimensions), while providing a basis for numerical work to explore, and hopefully resolve, the issue of the lower critical dimension. Finally, it helps to emphasize fundamental differences between phase transitions in spin glasses as opposed to more conventional systems such as ferromagnets.

Two different representations, each involving two replicas, were used to apply an FK type formalism—the Chayes–Machta–Redner(CMR) [13, 14] representation and the two-replica FK (TRFK) representation previously considered by Newman–Stein [15]. It is likely that other representations can also be used, as long as they involve the overlap of independent replicas. While various details will differ, as described in the text, the essential—and somewhat surprising—feature appears to be that the spin glass transition coincides with the emergence of percolating clusters of unequal densities.

Numerical results for the $d = 3$ EA spin glass seem to indicate that this occurs, as T is lowered below T_c, as the breaking of symmetry in the equal densities of both doubly occupied TRFK and blue CMR clusters that already percolate *above* the transition temperature. For the SK model, on the other hand, what occurs just above T_c is representation-dependent: in the TRFK representation, there is no doubly occupied percolation at all above T_c, while in the CMR representation there are two equal-density blue clusters just above T_c, similar to the situation in the $d = 3$ EA model. This difference in behavior above T_c may arise from the peculiarities of the SK model, and a similar representation-dependence may not occur in short-range models.

Finally, we speculate about the nature of the lower critical dimension. Our numerical results are consistent with prior studies [30, 33] indicating the appearance of broken spin-flip symmetry in the EA model in three dimensions. If the percolation signature scenario proposed here is correct for short-range models, it would help explain why there is no spin glass transition leading to broken spin-flip symmetry on simple planar lattices: two dimensions

does not generally provide enough "room" for two disjoint infinite clusters to percolate. However, a system that is infinite in extent in two dimensions but finite in the third might be able to support two percolating clusters, with unequal densities at low temperature. This and other possibilities will be explored in future work.

Acknowledgements We thank the Aspen Center for Physics where some of this work was performed. J.M. was supported in part by NSF DMR-0242402. He thanks New York University and Alan Sokal for hosting his sabbatical during which time this work was begun. C.M.N. was supported in part by NSF DMS-0102587 and DMS-0604869. D.L.S. was supported in part by NSF DMS-0102541 and DMS-0604869. Simulations were performed on the Courant Institute of Mathematical Sciences computer cluster.

References

1. Edwards, S., Anderson, P.W.: Theory of spin glasses. J. Phys. F **5**, 965–974 (1975)
2. Sherrington, D., Kirkpatrick, S.: Solvable model of a spin glass. Phys. Rev. Lett. **35**, 1792–1796 (1975)
3. Marinari, E., Parisi, G., Ricci-Tersenghi, F., Ruiz-Lorenzo, J.J., Zuliani, F.: Replica symmetry breaking in spin glasses: theoretical foundations and numerical evidences. J. Stat. Phys. **98**, 973–1047 (2000)
4. Newman, C.M., Stein, D.L.: Topical review: ordering and broken symmetry in short-ranged spin glasses. J. Phys.: Condens. Matter **15**, R1319–R1364 (2003)
5. Binder, K., Young, A.P.: Spin glasses: experimental facts, theoretical concepts, and open questions. Rev. Mod. Phys. **58**, 801–976 (1986)
6. Kasteleyn, P.W., Fortuin, C.M.: Phase transitions in lattice systems with random local properties. J. Phys. Soc. Jpn. (Suppl.) **26**, 11–14 (1969)
7. Fortuin, C.M., Kasteleyn, P.W.: On the random-cluster model, I: introduction and relation to other models. Physica **57**, 536–564 (1972)
8. Aizenman, M., Chayes, J.T., Chayes, L., Newman, C.M.: The phase boundary in dilute and random Ising and Potts ferromagnets. J. Phys. A Lett. **20**, L313–L318 (1987)
9. Imbrie, J., Newman, C.M.: An intermediate phase with slow decay of correlations in one dimensional $1/|x-y|^2$ percolation, Ising and Potts models. Commun. Math. Phys. **118**, 303–336 (1988)
10. Sweeny, M.: Monte Carlo study of weighted percolation clusters relevant to the Potts model. Phys. Rev. B **27**, 4445–4455 (1983)
11. Swendsen, R.H., Wang, J.-S.: Nonuniversal critical dynamics in Monte Carlo simulations. Phys. Rev. Lett. **58**, 86–88 (1987)
12. Wolff, U.: Collective Monte Carlo updating for spin systems. Phys. Rev. Lett. **62**, 361–364 (1989)
13. Chayes, L., Machta, J., Redner, O.: Graphical representations for Ising systems in external fields. J. Stat. Phys. **93**, 17–32 (1998)
14. Redner, O., Machta, J., Chayes, L.F.: Graphical representations and cluster algorithms for critical points with fields. Phys. Rev. E **58**, 2749–2752 (1998)
15. Newman, C.M., Stein, D.L.: Short-range spin glasses: results and speculations. In: Bolthausen, E., Bovier, A. (eds.) Spin Glasses. Lecture Notes in Mathematics, vol. 100, pp. 159–175. Springer, Berlin (2007)
16. Burton, R.M., Keane, M.: Density and uniqueness in percolation. Commun. Math. Phys. **121**, 501–505 (1989)
17. Gandolfi, A., Keane, M., Newman, C.M.: Uniqueness of the infinite component in a random graph with applications to percolation and spin glasses. Probab. Theory Relat. Fields **92**, 511–527 (1992)
18. Aizenman, M., Bricmont, J., Lebowitz, J.L.: Percolation of the minority spins in high-dimensional Ising models. J. Stat. Phys. **49**, 859–865 (1987)
19. Swendsen, R.H., Wang, J.-S.: Replica Monte Carlo simulations of spin glasses. Phys. Rev. Lett. **57**, 2607–2609 (1986)
20. Wang, J.-S., Swendsen, R.H.: Low temperature properties of the $\pm J$ Ising spin glass in two dimensions. Phys. Rev. B **38**, 4840–4844 (1988)
21. Wang, J.-S., Swendsen, R.H.: Replica Monte Carlo simulation (revisited). Prog. Theor. Phys. Suppl. **157**, 317–323 (2005)
22. Edwards, R.G., Sokal, A.D.: Generalizations of the Fortuin–Kasteleyn–Swendsen–Wang representation and Monte Carlo algorithm. Phys. Rev. D **38**, 2009–2012 (1988)
23. Houdayer, J.: A cluster Monte Carlo algorithm for 2-dimensional spin glasses. Eur. Phys. J. B **22**, 479–484 (2001)

24. Jörg, T.: Cluster Monte Carlo algorithms for diluted spin glasses. Prog. Theor. Phys. Suppl. **157**, 349–352 (2005)
25. Jörg, T.: Critical behavior of the three-dimensional bond-diluted Ising spin glass: finite-size scaling functions and universality. Phys. Rev. B **73**, 224431 (2006)
26. Machta, J., Newman, M.E.J., Chayes, L.B.: Replica-exchange algorithm and results for the three-dimensional random field Ising model. Phys. Rev. E **62**, 8782–8789 (2000)
27. Coniglio, A., Klein, W.: Clusters and Ising critical droplets: a renormalisation group approach. J. Phys. A: Math. Gen. **13**, 2775–2780 (1980)
28. Coniglio, A., di Liberto, F., Monroy, G., Peruggi, F.: Cluster approach to spin glasses and the frustrated-percolation problem. Phys. Rev. B **44**, 12605–12608 (1991)
29. de Arcangelis, L., Coniglio, A., Peruggi, F.: Percolation transition in spin glasses. Europhys. Lett. **14**, 515–519 (1991)
30. Katzgraber, H.-G., Körner, M., Young, A.P.: Universality in three-dimensional Ising spin glasses: a Monte Carlo study. Phys. Rev. B **73**, 224432 (2006)
31. Bollobás, B.: Random Graphs, 2nd edn. Cambridge University Press, Cambridge (2001)
32. Erdös, P., Rényi, E.: On the evolution of random graphs. Magyar Tud. Akad. Mat. Kutató Int. Közl **5**, 17–61 (1960)
33. Ballesteros, H.G., Cruz, A., Fernandez, L.A., Martin-Mayor, V., Pech, J., Ruiz-Lorenzo, J.J., Tarancon, A., Tellez, P., Ullod, C.L., Ungil, C.: Critical behavior of the three-dimensional Ising spin glass. Phys. Rev. B **62**, 14237–14245 (2000)